

Instrumental developments and recent experiments in near-field optical microscopy

H. Heinzelmann^a, Th. Lacoste^a, Th. Huser^a, H.J. Güntherodt^a, B. Hecht^b, D.W. Pohl^b

^a *Institute of Physics, University of Basel, Klingelbergstr. 82, 4056 Basel, Switzerland*

^b *IBM Research Laboratory, Säumerstr. 4, 8803 Rüschlikon, Switzerland*

Abstract

Recent advances in the understanding of light propagation in small dimensions as well as in instrumentation make scanning near-field optical microscopy (SNOM) a very promising tool for studying optical phenomena on a nanometer scale.

In this talk, we will demonstrate experiments carried out with the recently developed tunneling near-field optical microscope. We found superior image contrast, as compared with images taken with conventional aperture SNOM, along with the high resolution commonly achieved with fiber probes. This work was motivated by the theoretical investigations presented in Dr. Pohl's talk.

We will further describe two recently built instruments. The first is a scanning tunneling optical microscope combined with a scanning force microscope. The second instrument is an aperture-type SNOM mounted on the sample stage of a conventional inverted optical microscope. Of particular interest to us is imaging with polarization contrast. One of the goals is to study liquid-crystal films which have been micro-patterned with the help of a force microscope tip. These samples are promising as waveguides and potential electro-optical devices. Additionally, they represent very convenient test samples for polarization SNOM.

Keywords: Optical spectroscopy; Light scattering; Nanostructures

1. Introduction

The two most prominent representatives of near-field optical microscopes are the scanning near-field optical microscope (SNOM) and the scanning tunneling optical microscope (STOM) (also called the photon scanning tunneling microscope (PSTM)). SNOM [1–3] is often performed with aperture-type optical probes, i.e. the probing light is forced through a narrow (sub-wavelength) opening in an otherwise opaque material. Usually these optical probes are the pointed ends of optical fibers, obtained by heating and pulling, with metal (Al) evaporated from the sides. The uncoated spot at the apex measures about 30–100 nm in diameter. The high resolution is achieved by the imposed material constraint, of course in combination with a small working distance above the sample surface.

In STOM [4–7], on the other hand, a non-radiating (evanescent) field is generated at the sample surface, which is then tapped by a probe which is not necessarily of the aperture type. This evanescent field depends exponentially on the distance to the surface, and is additionally modulated by the sample surface. The principle of operation of STOM is analogous to that of the electron STM, thus the term STOM or

also PSTM is used (for photon scanning tunneling microscopy).

The concepts of SNOM are discussed in detail in Dr. Pohl's lecture [8]. In this paper we will describe three different set-ups of near-field optical microscopes. The first set-up has been developed at IBM Zurich and can be looked at as a combination of the schemes of SNOM and STOM. The other two set-ups describe instruments of the SNOM type and of the STOM type, as they were recently constructed in Basel.

2. Forbidden light SNOM

In an effort to combine the advantages of the two schemes outlined above, we have developed a new SNOM set-up [9–11]. Additionally motivated by two-dimensional calculations of the SNOM tip-sample geometry [12], we have started to record light at emission angles which are classically not allowed (Fig. 1). These calculations suggest that not only the intensity peaks at an angle of approximately 55° (which has to be compared with the much smaller angle of total internal reflection at the glass/air interface of 42°), but also the change in intensity when a sample is scanned is largest at this angle.

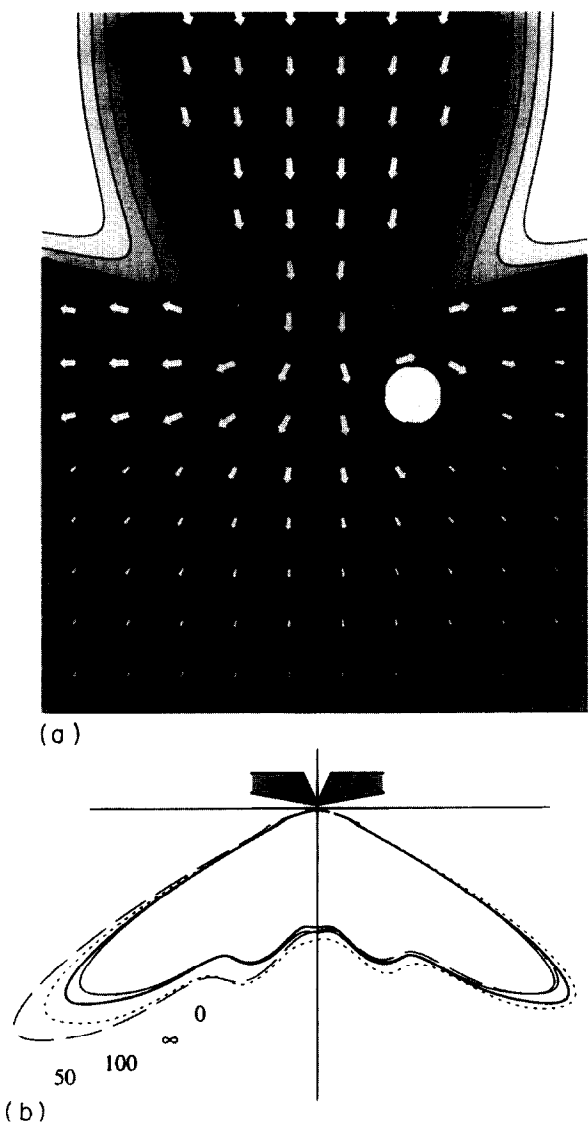


Fig. 1. MMP simulation of a SNOM fiber tip over a metallic sample. (a) The grey scale is a measure for the E field strength squared, white arrows indicate the pointing vector. (b) shows the emission distribution and its change as the sample is scanned. The maximum of the emission as well as the maximum change occur at an angle of 55° , a direction that is classically forbidden. From Ref. [12].

The set-up of this forbidden light SNOM is shown in Fig. 2. The sample is illuminated by an aperture-type fiber probe, as in conventional SNOM. But here we detect the light coupled via evanescent waves (photon tunneling) into the object if the gap width is smaller than approximately one wavelength. These contributions are transmitted at angles larger than the critical one and therefore cannot be seen with a regular aperture SNOM: they require an object carrier of, e.g., hemispherical shape. The transmission is strongly gap-width dependent (inset, F) and usually provides better contrast than the regular aperture SNOM mode (inset, A).

In near-field optical imaging, the tip-sample distance should be kept constant to separate pure optical contrast from effects induced by changes in the separation between the probe tip and sample surface. The distance can in principle

be regulated via the intensity of the forbidden light, however it is advantageous to use non-optical distance regulation because topographic and optical information can then be decoupled. For this purpose a technique based on shear force detection has been introduced [13,14], which is similar to dynamic scanning force microscopy (SFM). The only difference is that here a lateral vibration of the probe is used to measure the force between tip and sample, in contrast to a vertical oscillation in SFM. We have implemented an interferometric deflection sensor similar to the one described in Ref. [15], which to our experience is superior to the diffracted beam detection usually employed [11]. This distance control set-up can be routinely operated with excitation amplitudes of 2 nm peak-to-peak and less.

This microscope thus provides three different types of data simultaneously: forbidden light, conventional (forward) SNOM light, and surface topography (via shear force feedback).

To assess the obtainable resolution, we have imaged a test pattern made available to us by U. Fischer from the University of Münster. It is fabricated by evaporating Al onto an ordered

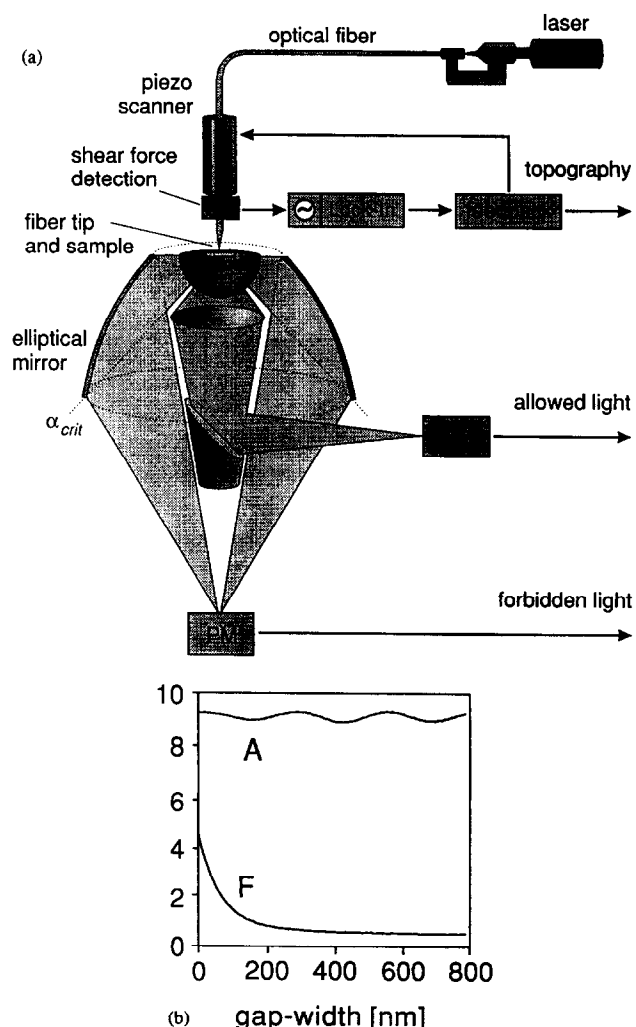


Fig. 2. (a) Set-up of the forbidden light SNOM. (b) Inset: approach curves for forbidden light (F) and allowed light (A). From Ref. [11].

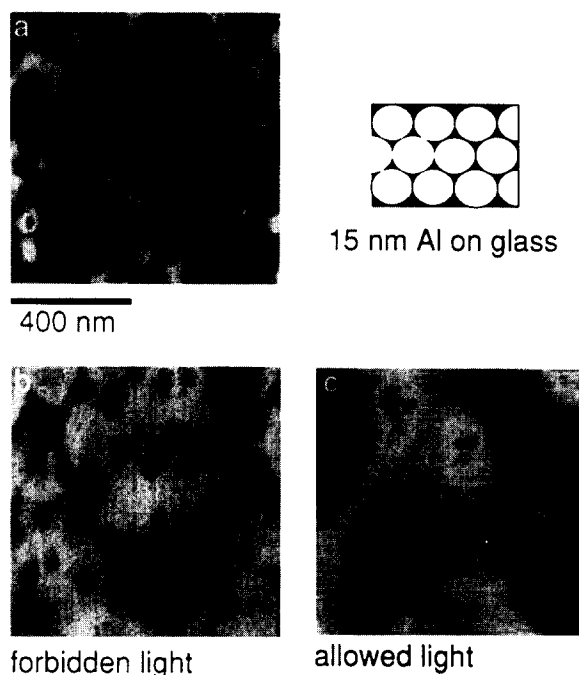


Fig. 3. Imaging of a latex sphere shadow mask, shown schematically in the inset in (a) (sample from U. Fischer, University of Münster). Topography (a) and forbidden light (b) clearly show the triangular shape of the metal patches; the allowed light signal in (c) is blurred, the structure is only faintly recognizable. From Ref. [11].

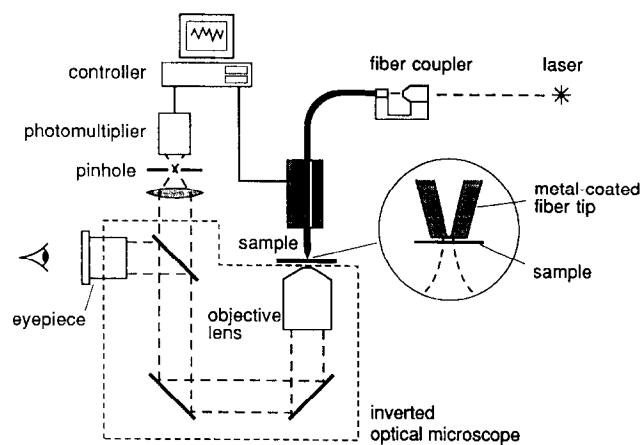


Fig. 4. Set-up of SNOM combined with a conventional optical microscope. From Ref. [16].

array of latex spheres of known diameter. The latex spheres are subsequently removed and a pattern from regularly shaped metal islands (15 nm thick, about 50 nm in size) remains on the surface. Fig. 3 shows images of this structure: (a) surface topography, (b) the forbidden light, and (c) the allowed (conventional SNOM) light. The forbidden light image shows superior contrast as compared with the conventional SNOM image. A resolution of approximately 50 nm is obtained.

3. Workhorse SNOM for imaging

We have set up a workhorse near-field optical microscope which is well suited for imaging of heterogeneous sample

surfaces. This microscope is built onto the sample stage of a conventional optical microscope, so that we can freely choose the location at which we perform SNOM imaging [16]. It is equipped with fluorescence and polarization contrast to fully exploit the richness of optical imaging. Shear force imaging additionally provides an image of the sample topography. The microscope is thus best suited for imaging, e.g., biological samples. The set-up is shown in Fig. 4.

As a first test sample we have chosen a pattern of approximately 15 nm high and 0.5 μm wide Cr squares arranged in a checker-board like fashion onto a glass substrate (Fig. 5). This structure has been provided by M. Fujihira from the Tokyo Institute of Technology. The topography (Fig. 5(a)) and near-field optical signal in transmission (Fig. 5(b)) were acquired simultaneously. Due to contrast reversal which is sometimes observed in shear force imaging, the Cr squares appear as dark depressions in the topography, as opposed to protrusions. This contrast reversal is likely due to strongly varying adhesive interactions when scanning the tip across glass/Cr boundaries, as observed with conventional force microscopy [16]. In the optical image the Cr squares appear dark, due to larger absorption of the metal. Sub-wavelength optical resolution could be demonstrated on another (non-patterned) glass surface where structures less than 100 nm apart could be imaged (Fig. 5(c)).

One of the main directions we will follow in the future is imaging with polarization contrast. An ideal test sample for these purposes are arrays of liquid-crystal domains, which

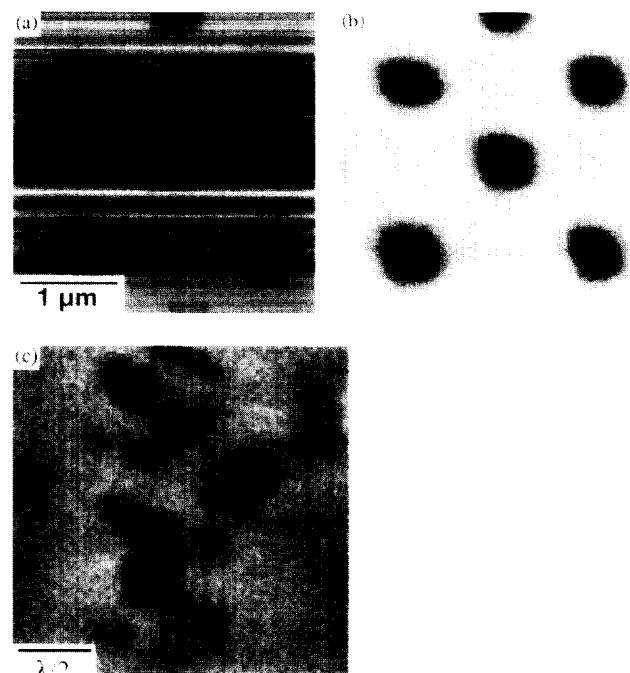


Fig. 5. Images of a Cr pattern on a glass substrate: (a) topography as provided by the shear force signal; due to contrast reversal, the Cr patches are observed as dark areas; (b) SNOM signal in transmission; the Cr patches appear dark due to higher absorption (the intensity range is 0.5 nW). (sample provided by M. Fujihira, Tokyo Institute of Technology); (c) SNOM image of some other structure on a glass surface; features less than 100 nm apart can be distinguished.

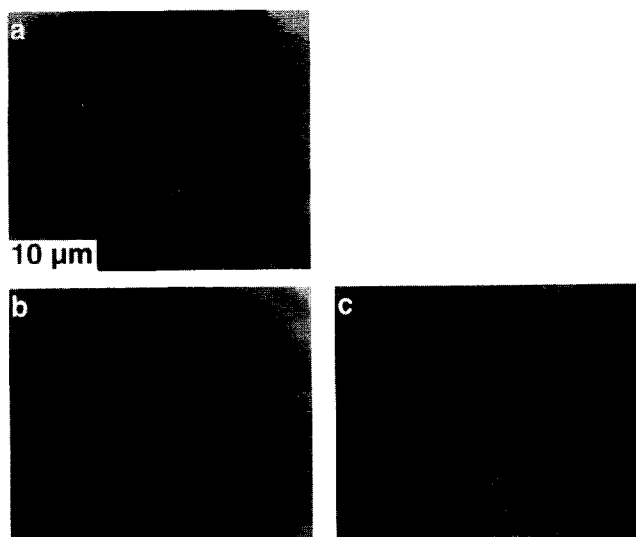


Fig. 6. Polarization contrast on a liquid crystal array grating as described in Ref. [17]. Topography (a) and SNOM images with analyzer adjusted for maximum (b) and minimum (c) transmission. Although the grating is only faintly visible in (c), a reversed contrast with respect to (b) can be observed.

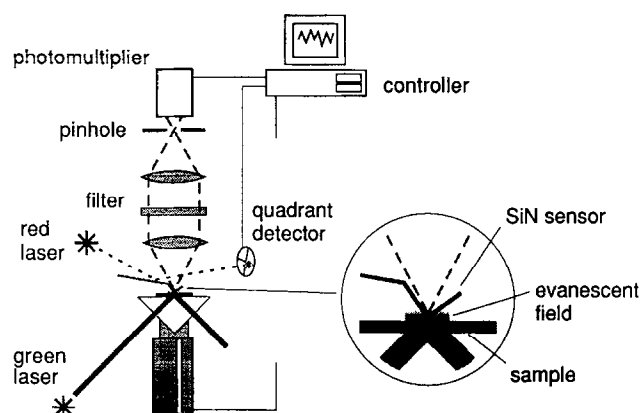


Fig. 7. Set-up of STOM combined with a force microscope. Green laser light is generating an evanescent field at the sample surface, which is scattered at the force sensor tip and detected with a photomultiplier tube. From Ref. [16].

could recently be fabricated by microscratching with a force microscope [17]. Fig. 6 shows the topography (a) and the

optical images for two different analyzer settings, set for minimum (b) and maximum (c) transmission of light at an arbitrary point over the sample surface. While at this stage this is a rather qualitative setting, the acquired optical images show different contrast, the recorded topography is identical and assures us that the observed differences are not due to sample drift.

4. Combined optical tunneling/force microscope

A further development is the combination of a scanning tunneling optical microscope (STOM) and a scanning force microscope (SFM) [16,18]. In this instrument, the tip of the SFM cantilever acts as a scattering center that disturbs the evanescent field above the sample [19,20], much in the same way as the bare optical fiber tip described above. In a STOM scheme the optical resolution is not determined by the smallness of optical apertures, which is limited by the penetration depth of the metal coating. Rather, as a scattering scheme, it carries the potential for higher spatial resolution, since even a single atom can act as a scattering center. To aid the interpretation of the optical data, it is a great advantage to simultaneously acquire a force topograph of the sample surface.

The set-up is shown in Fig. 7. The transparent sample is optically contacted to a glass prism which is mounted on an xyz piezoscanner. The prism is illuminated by a green HeNe laser ($\lambda = 543.5 \text{ nm}$), the light undergoes total internal reflection inside the prism and generates an evanescent field above the sample. A standard force microscope tip acts as a scattering center, and the scattered light is collected at the back of the cantilever from which the metal coating has been removed by etching in King's water ($3\text{HCl} + \text{HNO}_3$). The light intensity that reaches the photomultiplier tube is typically 0.25 nW .

One of the first images obtained with this instrument is shown in Fig. 8 [16,18]. We found a dirt particle on the sample-carrying glass prism which we scanned in constant force mode, the scan size is approximately $1 \mu\text{m}^2$. The sample topography (Fig. 8(a)) shows a particle height of approximately 92 nm . A more detailed structure of the particle can

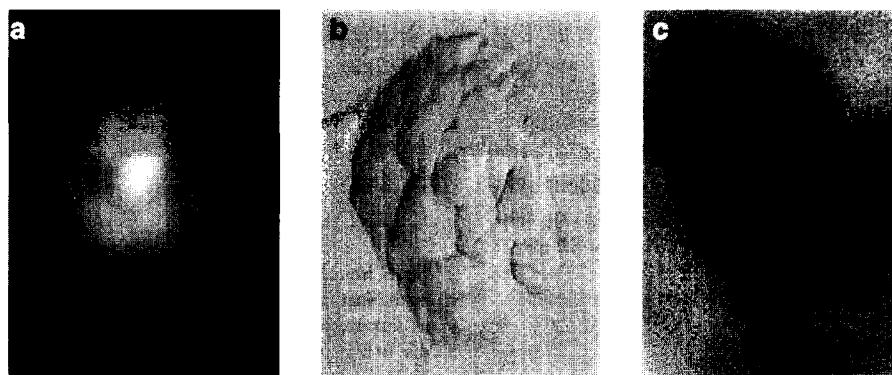


Fig. 8. STOM and SFM images of a particle on a glass surface, (a) normal force (topography), (b) lateral force (friction), and (c) optical signal. From Ref. [16].

be seen in the lateral force image (Fig. 8(b)) which is often the case due to an apparent edge enhancement. Some of this surface structure is also observed in the near-field optical image (Fig. 8(c)), although with less resolution. The highest point of the grain has the least light intensity. The whole picture is superposed by light scattered and diffracted by the grain.

5. Summary and outlook

We have set up various schemes for near-field optical microscopy which are capable of sub-wavelength resolution. The aim of most of these developments is to assess more fundamental rather than applied questions of near-field optical microscopy, such as emission properties from miniature optical probes, or the limits of resolution of near-field optical microscopy. Our understanding of the technique is not yet exhaustive, but still there are many applications (such as semiconductors and biology) where it proves extremely valuable due to its variety of observable contrasts. An even bigger impact can be anticipated when smaller and more reducible optical probes, e.g. by microfabrication, are available.

Acknowledgements

We are grateful to L. Novotny (Swiss Federal Institute of Technology (ETH), Zürich) for useful discussions. Test samples were kindly provided by U.Ch. Fischer (University of Münster), M. Fujihira (Tokyo Institute of Technology) and M. Rüetschi (University of Basel). The work has been financially supported in part by the Swiss Priority Program Optique and the Swiss National Science Foundation.

References

- [1] D.W. Pohl, W. Denk and M. Lanz, *Appl. Phys. Lett.*, **44** (1984) 651.
- [2] E. Betzig and J. Trautman, *Science*, **257** (1992) 189.
- [3] H. Heinzelmann and D.W. Pohl, *Appl. Phys. A*, **59** (1994) 89–101.
- [4] F. de Fornel, J.P. Gouffonnet, L. Salomon and E. Lesniewska, *Proc. SPIE*, **1139** (1989) 77.
- [5] D. Courjon, K. Sarayeddine and M. Spajer, *Opt. Commun.*, **71** (1989) 23.
- [6] R.C. Reddick, R.J. Warmack and T.L. Ferrell, *Phys. Rev. B*, **39** (1989) 767.
- [7] N.F. van Hulst, F.B. Segerink and B. Bölger, *Opt. Commun.*, **87** (1992) 212.
- [8] D.W. Pohl, *Thin Solid Films*, in press.
- [9] B. Hecht, H. Heinzelmann and D.W. Pohl, *Ultramicroscopy*, **57** (1995) 228.
- [10] H. Heinzelmann, B. Hecht, L. Novotny and D.W. Pohl, *J. Microsc.*, **177** (1994) 115.
- [11] B. Hecht, H. Heinzelmann, D.W. Pohl and L. Novotny, in O. Marti and R. Möller (eds.), *NATO Series E: Photons and Local Probes*, Kluwer, Dordrecht, in press.
- [12] L. Novotny, D.W. Pohl and P. Regli, *J. Opt. Soc. Am. A*, **11** (1994) 1768.
- [13] R. Toledo-Crow, P.C. Yang, Y. Chen and M. Vaez-iravani, *Appl. Phys. Lett.*, **60** (1992) 2957.
- [14] E. Betzig, P.L. Finn and S.J. Weiner, *Appl. Phys. Lett.*, **60** (1992) 2484.
- [15] D. Rugar, H.J. Mamin, R. Erlandsson, J.E. Stern and B.D. Terris, *Rev. Sci. Instrum.*, **59** (1988) 2337.
- [16] Th. Lacoste, Th. Huser, H. Heinzelmann and H.-J. Güntherodt, in O. Marti and R. Möller (eds.), *NATO Series E: Photons and Local Probes*, Kluwer, Dordrecht, in press.
- [17] M. Rüetschi, P. Grütter, J. Fünfschilling and H.-J. Güntherodt, *Science*, submitted.
- [18] Th. Huser, *Diploma Thesis*, University of Basel, 1994.
- [19] N.F. van Hulst, M.H.P. Moers, O.F.J. Noordman, R.G. Tack and F.B. Segerink, *Appl. Phys. Lett.*, **62** (1993) 461.
- [20] F. Baida, D. Courjon and G. Tribillon, in D.W. Pohl and D. Courjon (eds.), *Proc. NFO I: Near Field Optics*, NATO ASI Series E, Vol. 242, p. 71, 1993.